Increased likelihood of compound dry and hot extremes in India

Ravi Kumar Guntu, Bruno Merz, Ankit Agarwal

PII: S0169-8095(23)00186-2

DOI: https://doi.org/10.1016/j.atmosres.2023.106789

Reference: ATMOS 106789

To appear in: *Atmospheric Research*

Received date: 25 January 2023

Revised date: 8 March 2023

Accepted date: 27 April 2023

Please cite this article as: R.K. Guntu, B. Merz and A. Agarwal, Increased likelihood of compound dry and hot extremes in India, *Atmospheric Research* (2023), https://doi.org/10.1016/j.atmosres.2023.106789

Increased likelihood of compound dry and hot extremes in India

Ravi Kumar Guntu[1,2], Bruno Merz[2] and Ankit Agarwal[1*]
[1]Department of Hydrology, Indian Institute of Technology Roorkee, Roorkee, 247667, India
[2]Section 4.4: Hydrology, GFZ German Research Centre for Geosciences, Potsdam 14473, Germany

*Corresponding author: ankit.agarwal@hy.iitr.ac.in

Abstract

Compound dry and hot extremes (CDHE) are periods of prolonged dry and hot weather. Their joint occurrence typically impacts society and nature stronger compared to the occurrence of the single hazards. Understanding the likelihood, variability and drivers of CDHE is challenging due to the complexity of the climate system involving interactions and feedbacks among atmosphere-land processes. In this study, we first investigate the role of the dependence between precipitation and temperature for the likelihood of CDHEs. We demonstrate that both the dependence strength and its type, i.e. the degree of tail dependence, substantially affect the CDHE likelihood. We then analyze the space-time variation of CDHE characteristics during the Indian Summer Monsoon across India for the period 1961-2014. We find strong negative association and substantial tail dependence between precipitation and temperature in some regions. Event coincidence analysis reveals that low soil moisture preconditioned by dry extremes is responsible for 55-65% of CDHE occurrence. Our analysis of the temporal evolution of CDHE characteristics finds an increasing negative association between precipitation and temperature leading to a 2 to 3-fold rise of CDHE frequency for some regions of India.

Keywords

Compound extremes, Dependence, Soil moisture, Indian summer monsoon, Event coincidence analysis, Climate change.

1 Introduction

The Indian summer monsoon (ISM) is a major source of precipitation in India, and its decline threatens the water security of more than a billion people (Mishra et al., 2022). Due to global warming, India has become more vulnerable to high-impact extremes, such as droughts and heatwaves (Jha et al., 2022; Kulkarni et al., 2020; Rawat et al., 2022). These events have become more frequent and intense and are anticipated to worsen in the future, which could result in food insecurity and economic instability (Gupta et al., 2020; Kathayat et al., 2022). The droughts can lead to increased evaporation rates due to the lack of moisture in the soil, which can exacerbate the drought conditions. Furthermore, the consequences of droughts can be more catastrophic when they coincide with heat extremes (Mukherjee et al., 2023; Yin et al., 2023). Therefore, it is crucial to comprehensively understand the likelihood of such extremes in India to manage them effectively under global warming.

The IPCC Special Report on Managing the Risks of Extreme Events and Disasters to Advance Climate Change Adaptation defined the simultaneous occurrence of any two extremes as a compound event (Seneviratne et al., 2012). Since then, many studies have investigated compound dry and hot events/extremes (CDHE) by applying multivariate statistics to observational and climate simulation data (Bevacqua et al., 2022; Meng et al., 2022; Ridder et al., 2021). In India, several CDHEs with a substantial reduction in agricultural productivity have occurred in the past 70 years, namely in 1951, 1972, 1979, 1987, 2009, 2014 and 2015 (Mishra et al., 2020b), and more frequent occurrences of CDHE are expected owing to climate change (Seneviratne et al., 2021). Therefore, understanding the characteristics and variability of CDHE during the ISM is of utmost importance.

Most previous studies have assessed CDHE by counting the simultaneous occurrences of dry and hot extremes, whereas dry and hot extremes are defined as events beyond a certain threshold (Meng et al., 2022; Wu et al., 2021). This counting approach quantifies CDHE frequency and spatial extent, but falls short in characterizing the precipitation-temperature (P-T) dependence (Wu et al., 2020). Considering P (for precipitation) and T (for temperature), CDHE can be characterized by the probability $Pr(P \leq p \cap T > t)$, where p and t are the thresholds of P and T defining the extreme event. This joint probability can be inferred either empirically or parametrically. The empirical approach utilizes plotting position formulas that are based on the number of paired occurrences for the period of interest (Hao and AghaKouchak, 2014). The parametrical approach builds on the marginal distributions of precipitation and temperature and on their dependence (Genest and Favre, 2007). The empirical approach is easy to apply and free from fitting the parametric distributions, thereby alleviating the computational burden (Hao and AghaKouchak, 2014). However, it cannot be used for extrapolating beyond observed values, and, in addition, it cannot quantify the P-T dependence (Raymond et al., 2020).

The P-T dependence needs however to be considered, as globally dry (wet) summers tend to be associated with hot (cool) conditions (Trenberth et al., 2014). Similarly,

Zscheischler & Seneviratne (2017) reported a significant negative P-T dependence during the hottest 3-month period using observational and climate model simulations across the globe. This negative dependence has been explained by land-atmosphere interactions (Berg et al., 2015; Miralles et al., 2019). Precipitation deficits lead to soil moisture depletion, which in turn reduces evapotranspiration. This reduction in latent heat flux is largely counterbalanced by increasing sensible heat flux and upwelling longwave radiation, both of which are associated with higher surface temperature (Berg et al., 2016). Therefore, soil moisture-temperature coupling been identified as one of the main drivers of CDHE (Osman et al., 2022; Schumacher et al., 2022). Furthermore, Hao and Singh, (2020) highlighted that the P-T dependence might fluctuate under climate change, impacting the likelihood of CDHE. These studies demonstrate the need for a comprehensive assessment to understand the relationship between CDHE likelihood and P-T dependence.

The Indian subcontinent has experienced regional droughts and heatwaves since the start of the 21st century, resulting in catastrophic impacts on society and ecosystems (Das et al., 2022; Ganguli, 2023). These climate-related hazards have resulted in economic losses of $80 billion between 1998 and 2017 and countless irreparable human losses (Wallemacq et al., 2018). Research by Mishra et al., (2020b) has shown that crop yields were significantly reduced by 146 and 111 kg/ha due to compound dry and hot summers in 1987 and 2009, respectively. Sharma and Mujumdar, (2017) reported an increasing frequency and spatial extent of CDHE at weekly time scale. Additionally Guntu and Agarwal, (2021) have reported a threefold increase in CDHE frequency for the recent period (1977–2019) relative to the base period (1951–1976), exhibiting a strong spatial pattern. Despite these important findings, there is a research gap in understanding the changes in the likelihood of compound dry and hot extremes during the Indian summer monsoon, particularly regarding intra-seasonal variability. To the authors' knowledge, this is the first study to investigate the impact of P-T dependence on the likelihood of CDHE occurrence during the Indian summer monsoon.

Copulas are multivariate statistical distributions that provide a straightforward parametric approach to modelling the dependence between random variables (Genest and Favre, 2007). Recently, copulas have emerged as a preferred approach to model the P-T dependence at regional and global scales (Tootoonchi et al., 2022). Employing copulas, Zscheischler & Seneviratne, (2017) proposed the Likelihood Multiplication Factor (LMF) to quantify the change in CDHE likelihood when the P-T dependence is considered. Recent studies (Aihaiti et al., 2021; Ridder et al., 2020) have successfully applied LMF and found it helpful to assess the variability of CDHE at different spatial and temporal scales. However, further investigation is required to understand how different copula families and extreme levels affect LMF variation. In this paper, we build on these recent methodological advances to investigate the space-time variations of CDHE likelihood during the Indian summer monsoon. We first investigate how the nature of dependence, that is whether there is tail dependence, affects LMF. We then analyze the spatial and temporal variation of CDHE likelihood during ISM (June, July, August, and September, JJAS) across India for the period 1961-2014.

2 Data and Methods

2.1 Data

We use gridded monthly precipitation and temperature of the Indian mainland (between $68^0E - 98^0E$ and $8^0N - 37^0N$) from 1961 to 2014 provided by the University of Delaware (Willmott, 2000). To evaluate the role of soil moisture-temperature coupling, we use the gridded monthly soil moisture from the Climate Prediction Centre, NOAA (van den Dool, 2003). A link to access the data is provided in the data availability statement. Owing to the high relevance of the monsoon for agricultural production and water resource management, we focus on the ISM (June-September). Although there is substantial spatial variability in the mean annual precipitation (Fig. S1), most grid points receive $>70\%$ of the total annual precipitation during the ISM. To facilitate the discussion and interpret the results, based on previous studies (Guntu et al., 2020; Guntu and Agarwal, 2021), we divide the Indian mainland into ten sub-regions (Fig. 1), i.e., Western India (WI), North-western India (NWI), North-central India (NCI), Eastern India (EI), South-central India (SCI), South-eastern coastline (SEC), Konkan coast (KC), North-eastern India (NEI), Rain-belt Western Himalaya (RBWH) and Rain-shadow Western Himalaya (RSWH). To test the sensitivity of the results to the data used, we repeat the analysis with Bias-corrected Indian Meteorological Department (BIMD) data (Mishra et al., 2020a) and APHRODITE (Yatagai et al., 2012) (see data availability statement). These datasets have been used in various hydro-meteorological applications (Das et al., 2022; Kanda et al., 2020; Mallya et al., 2016) and are considered highly accurate and capable of capturing the spatiotemporal variability of precipitation and temperature over India.

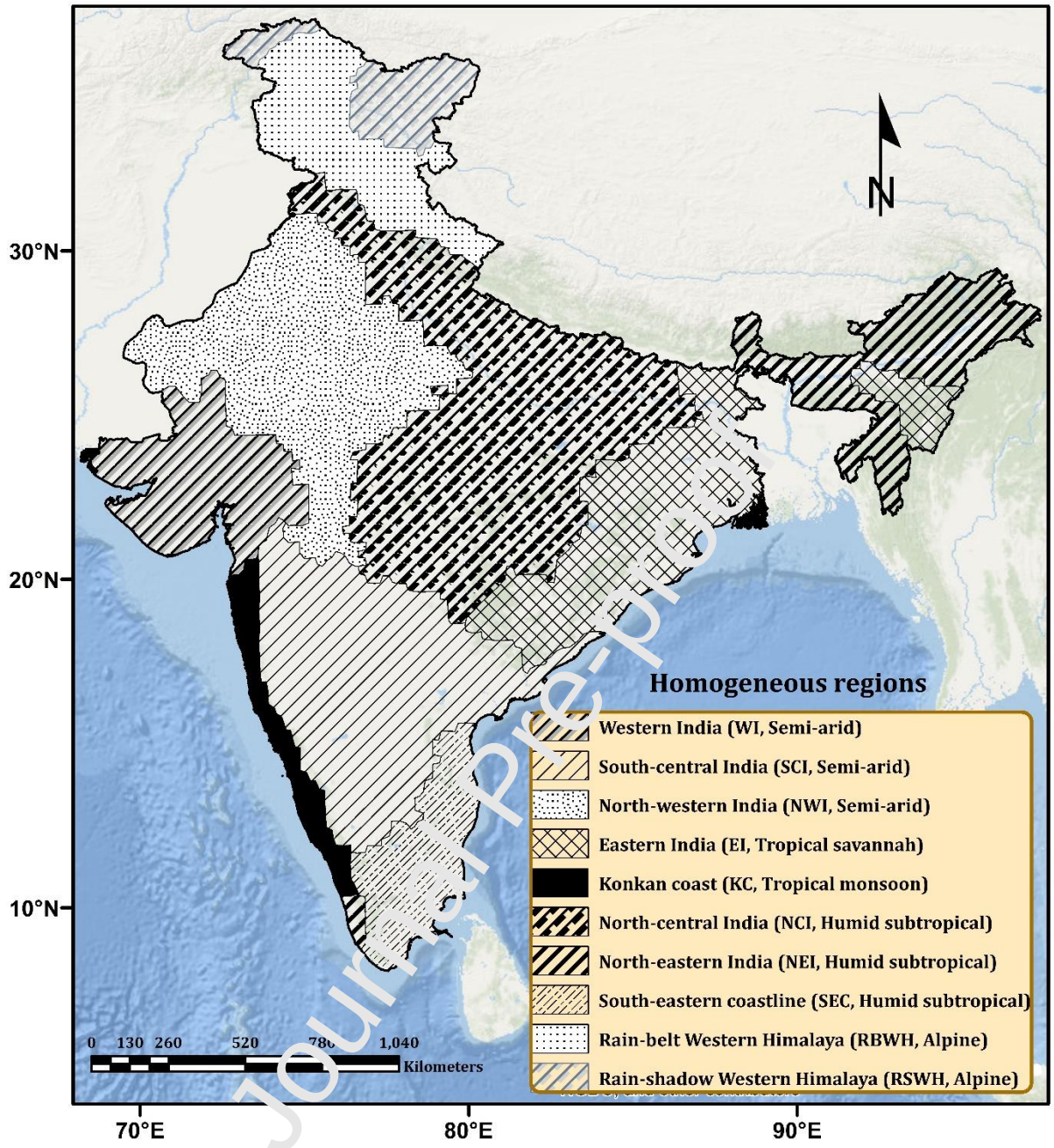

Figure 1: Sub-regions of the Indian mainland. Each region's name is displayed, and the type of climate regime is listed in parentheses.

2.2 Bivariate method to derive CDHE likelihood

Copulas have become a powerful tool for modeling the dependence of two continuous random variables and have been beneficial in separately modeling marginal and joint cumulative distribution functions (Ganguli and Merz, 2019; Zhang and Singh, 2019). The copula approach can construct the joint probability distribution flexibly in which the marginal distributions are independent of the dependence nature (Salvadori and De Michele, 2010). Consider two random variables P (for precipitation) and T (for Temperature) whose CDFs are defined as $p^* = F_P(p) = Pr(P \leq p)$ and $t^* = F_T(t) = Pr(T \leq t)$, respectively. The joint CDF of P and T with a copula function C is expressed as (Genest and Favre, 2007)

$$F_{(PT)}(p,t) = Pr(P \leq p, T \leq t) = C(p^*, t^*; \Theta) \quad (1)$$

Where Θ is the parameter of copula function and represents the strength of dependence. Using the marginal CDF, the CDHE likelihood in which precipitation is smaller than a certain threshold (u) and temperature is larger than the threshold (v) is calculated as (Zscheischler and Seneviratne, 2017)

$Pr(p^* \leq u \cap t^* > v) = u - C(u, v; \Theta)$ (2)

We model CDHE as simultaneous occurrence of precipitation with a non-exceedance probability of 0.20 and temperature with a probability of exceeding 0.80. These two thresholds are often used in the literature to define moderate CDHE (Hao et al., 2022; Wu et al., 2020), but other values ($u = 0.10, 0.30$ and $v = 0.90, 0.70$) are also used and similar results are achieved. According to scientific research, events where both variables are classified as moderately severe and above (Fig. S2) have adverse impacts (Mishra et al., 2020b).

Clayton, Frank, Gumbel, and Joe are widely used copula families for compound events. The Frank family is only able to capture the overall dependence, while the others express the tail dependence (Clayton: lower tail; Gumbel, Joe: upper tail). In our study, the tail dependence specifically refers to the dependence between the upper and lower tails of the variables (Tootoonchi et al., 2022). However, we acknowledge that the tail dependence has a specific definition in probability theory, which is related to the behavior of the joint distribution function as the variables approach their extreme values (Manoj et al., 2022). Since precipitation and temperature during the Indian monsoon season are negatively dependent (Trenberth and Shea, 2005), the traditional version of the Clayton, Gumbel and Joe families cannot be used. Instead, their 90-degree rotated transformed form can be applied (Nikoloulopoulos et al., 2012). We use these four families (see Table S1 for an overview) and select the best-fit family by means of the Bayesian Information Criterion (BIC). BIC accounts for both model complexity and the number of observations (Tootoonchi et al., 2022). We transform the marginal distributions into normalized ranks to obtain a uniform distribution in the marginals. This is a common approach if the best-fit family must be obtained when using copulas. The R package Vine copula is used to fit the copulas and marginal distributions and for model diagnostics (Schepsmeier et al., 2015).

2.3 Event Coincidence Analysis

We apply event coincidence analysis to evaluate the coincidence between two or three event series and test the hypothesis of statistical interdependencies among them (Donges et al., 2016; Manoj et al., 2022). For a grid point (X), monthly time series of temperature (T), soil moisture (SM) and precipitation (P) are converted into binary series where one denotes an occurrence of an event and zero denotes the absence of an event during the timestep. The T, SM and P monthly time series are represented by $X^T(t_i)$, $X^{SM}(t_j)$ and $X^P(t_k)$, respectively, with observations for each $t_i, t_j, t_k \in [1, T]$, where T denotes the last timestep of the observed record. The event time series $Y^T(t_i)$, $Y^{SM}(t_j)$ and $Y^P(t_k)$ are defined as:

$$Y^T(t_i) = \begin{cases} 1, & X^T(t_i) \geq \text{a} \\ 0, & else \end{cases} \quad (3)$$

$$Y^{SM}(t_j) = \begin{cases} 1, & X^{SM}(t_j) \leq \text{b} \\ 0, & else \end{cases} \quad (4)$$

$$Y^{P}(t_k) = \begin{cases} 1, & X^{P}(t_k) \leq \text{c} \\ 0, & else \end{cases} \quad (5)$$

a, b and c denote the site-specific percentile cutoff for T, SM and P considering the entire period (see Appendix A). We use the 80th percentile (a) to retain the hot extremes and the 20th percentile (b, c) for low soil moisture and dry extremes, respectively. Using the CoinCalc package developed by Siegmund et al., (2017), we first evaluate the hypothesis that hot extremes occur simultaneously as dry extremes using the precursor coincidence rate (P_{cr}). Utilizing the conditional precursor coincidence rate (CP_{cr}), we then test the hypothesis that hot extremes appear at the same time as low soil moisture if and only if dry extremes occurred simultaneously. P_{cr} and CP_{cr} are defined as (Donges et al., 2016; Siegmund et al., 2017):

$$P_{cr} = \frac{1}{N_T} \sum_{i=1}^{N_T} H\left(\sum_{k=1}^{N_P} I_{[0\ \Delta T]}(t_i^T - t_k^P) \right) \quad (6)$$

$$CP_{cr} = \frac{1}{N_T} \sum_{i=1}^{N_T} H\left(\sum_{j=1}^{N_{SM}} H\left(\sum_{k=1}^{N_P} I_{[0\ \Delta T]}(t_j^{SM} - t_k^P) \right) I_{[0\ \Delta T]}(t_i^T - t_j^{SM}) \right) \quad (7)$$

Where N_T, N_{SM} and N_P are the number of events in T, SM and P event series, respectively, occurring at times t_i^T, t_j^{SM} and t_K^P. ΔT is the temporal tolerance between the timing of the events. We use the instantaneous coincidence ($\Delta T = 0$), where $I()$ is the indicator function and $H()$ is the Heaviside function and their outputs are defined as follows:

$$I_{[0\ \Delta T]} = \begin{cases} 1, & t_i^T - t_k^P = 0 \\ o, & else \end{cases} \quad (8)$$

$$H = \begin{cases} 1, & \sum_{k=1}^{N_P} I_{[0\ \Delta T]}(t_i^T - t_k^P) > 0 \\ o, & else \end{cases} \quad (9)$$

The range of P_{cr} is zero to one. Zero implies that no hot extreme coincides with a dry extreme, and one represents the situation in which all hot extremes coincide with dry extremes. The procedure to calculate P_{cr} for a prototypical example is described in Manoj et al. (2022). CP_{cr} also varies between zero to one. Zero suggests that no hot extremes are triggered by low soil moisture pre-conditioned by dry extremes and one indicates that all the hot extremes appear simultaneously with low soil moisture pre-conditioned by dry extremes. Statistical significance is evaluated by generating an ensemble of 100O shuffle surrogate event series. We use a value of 0.05 as the significance level to reject the null hypothesis that the obtained coincidence is purely random (Donges et al., 2016; Siegmund et al., 2017).

3 Results and Discussion

3.1 Effect of dependence on CDHE likelihood

To quantify the effect of dependence on the likelihood, Zscheischler & Seneviratne (2017) defined the Likelihood Multiplication Factor (LMF) as the ratio of the probability of CDHE with dependence to the independent case. They illustrated the effect of dependence on the likelihood using the Frank copula. However, the Frank copula does not consider tail dependence. We extend their analysis by investigating how LMF varies with the nature of P-T dependence, that is, how LMF is affected by is upper/lower tail dependence. We illustrate the effect of dependence on LMF for different copula families. We generate synthetic samples consisting of 1167 pairs of precipitation and temperature values with uniform marginals for 30 values of the copula parameter Θ corresponding to Kendall rank correlation in the interval $[-0.9 - 0.01]$. 1167 are the number of precipitation and temperature grid points available on the Indian mainland, and 30 observations represent one climate normal (30 years). For each parameter value, we compute the CDHE likelihood and obtain LMF using Eq. 2. Figure 2 shows the theoretical variation of LMF with P-T dependence for different copula families. The uncertainty estimates presented in Fig. S3 were calculated based on 1167 sequences, which represent the number of grid points on the Indian mainland.

The P-T dependence strongly affects the likelihood of CDHE: With a higher (negative) dependence more CDHEs are expected to occur. For example, if precipitation and temperature are independent, the estimated number of CDHE in one climate normal period is one or two $[(0.2 - 0.2 \times 0.8) \times 30 = 1.2]$. However, if correlated with a value $\tau < -0.28$ and $\tau < -0.55$, the occurrence of CDHE increase two- and three-fold for the Frank copula, as shown in Fig. 2.

However, the number of CDHE is amplified or reduced based on the precipitation and temperature tail dependence. The Gumbel and Joe copulas, that is, their 90° rotated versions, show upper tail dependence. Hence, low precipitation values tend to occur with high temperature values, which translates into a higher likelihood of CDHE occurrence. Conversely, the likelihood of CDHE occurrence is lower when there is lower tail dependence between temperature and precipitation. Therefore, the strength and nature of the dependence, in terms of tail dependence substantially affect the likelihood of CDHE.

Moreover, the impact of dependence on LMF varies for different extreme levels and copula families. The extreme levels, represented by the pairs (u, v), indicate the level of rarity of the event of interest. When the level of extreme increases, the LMF also tends to increase. For example, a pair of (0.30,0.70) indicates an abnormal CDHE that occurs with a probability of 0.09 when the variables are independent. However, if the P-T dependence is correlated with a value $\tau < -0.28$ and $\tau < -0.55$, the occurrence of CDHE increase 1.65 and 2.28 times for the Frank copula (Fig. S4a). For the severe CDHE (0.10,0.90), the probability of occurrence is 0.01 when the variables are independent. But if correlated with a value $\tau < -0.28$ and $\tau < -0.55$, the occurrence of CDHE increase 2.29 and 4.08 times for the Frank copula (Fig. S4c).

Therefore, a higher negative P-T dependence increases the likelihood of CDHEs, and the tail dependence between precipitation and temperature also affects the likelihood of CDHE occurrence. Furthermore, the impact of dependence on the LMF varies for different extreme levels and copula families. As the level of extreme increases, the LMF tends to increase, and different copula families exhibit different results. The Frank copula, for instance, shows an increase in the occurrence of CDHEs with a higher negative dependence, while the Gumbel and Joe copulas exhibit upper tail dependence, leading to a higher likelihood of CDHE occurrence.

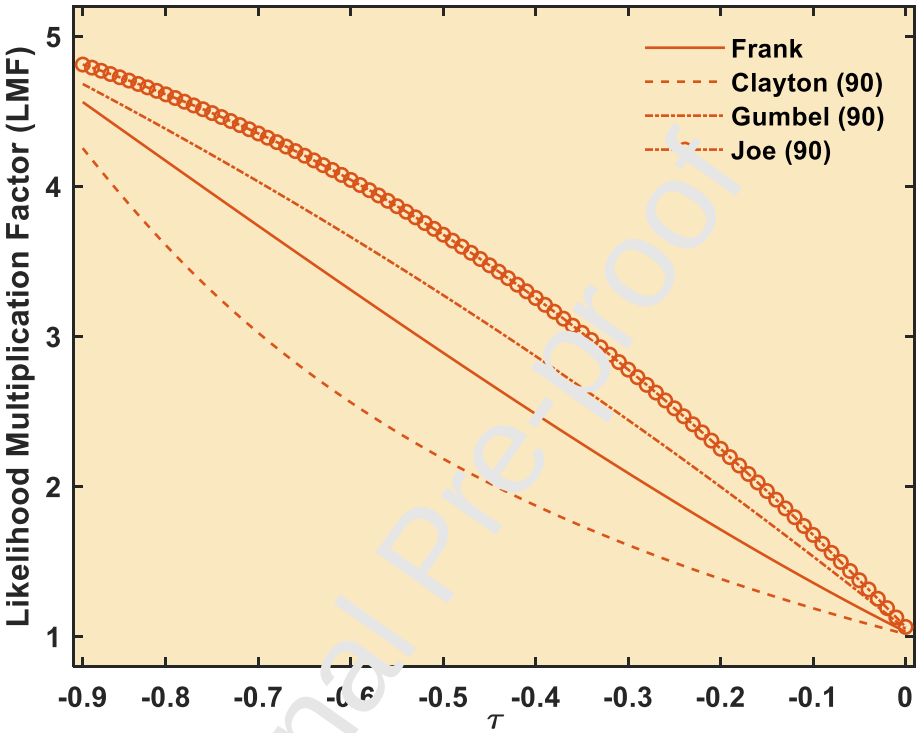

Figure 2: Effect of dependence on the Likelihood Multiplication Factor (LMF) for different copula families or their 90-degree rotated versions (90 in parentheses). The X-axis represents the P-T dependency in terms of Kendall rank correlation (τ), the Y-axis shows by which factor the probability of CDHE occurrence is increased when considering dependence compared to the independent case.

3.2 Spatial variation of CDHE likelihood

We calculate Kendall's Tau (τ) between the marginals of precipitation and temperature using observed monthly total precipitation and mean temperature during ISM for the period 1961-1990. The WMO recommends 1961-1990 to monitor climate change and views it as a stable reference period (Trenberth et al., 2014). τ during ISM (JJAS) varies considerably between -0.66 and 0.38 across India (Fig. 3a-d). Most grid points and sub-regions (see boxplots in Fig. 4a) have a negative association between precipitation and temperature. The analysis reveals clear spatial patterns in the dependence between precipitation and temperature during the ISM season, which varies considerably across India. The negative association between precipitation and temperature suggests that an increase in temperature leads to a decrease in precipitation, which is a common feature of monsoon climate (Dash and Maity, 2023). In June (Fig. 3a), we find stronger negative dependence in Eastern India, Western India, North-central India, Konkan coast and North-eastern India with median correlation of -0.46, -0.40, -0.39, -0.38 and -0.37, respectively (Fig. 4). However, Little dependence is found in South-eastern coastlines,

South-central India and Western Himalayas (Fig. 3a). The stronger negative correlation observed in June suggests that these regions are more susceptible to reduced precipitation due to higher temperatures. This could be attributed to a combined effect of local and large-scale circulation patterns, such as the thermal contrast between land and ocean , the Western Himalayan mountains, and the Indian Ocean Dipole (IOD) mode (Hrudya et al., 2021; Oza et al., 2022). For instance, Sankar et al., (2021) reported that Eastern India is known to be influenced by the Bay of Bengal branch of the monsoon, which is sensitive to sea surface temperature (SST) anomalies, while Western India is influenced by the Arabian Sea branch, which is modulated by the IOD mode.

In July (Fig. 3b), a high negative correlation is seen across the North-Western and Western India with median correlation of -0.36 and -0.32, which could be due to the weakening of the monsoon circulation and the suppression of precipitation by an atmospheric high-pressure system over the region (Bhatla et al., 2016; Vázquez et al., 2023). Compared to July, the negative dependence during August (Fig. 3c) was more pronounced on the Konkan coast and North-central India with a median correlation of -0.36 and -0.32, respectively. Navale and Karthikeyan, (2023) reported that the westward shift of the monsoon trough is responsible for the weakening of the monsoon circulation. In September, a high negative dependence is found over North-western India and Western India with median correlation of -0.48 and -0.40, respectively. This could be attributed to the withdrawal of the monsoon and the increasing influence of westerly disturbances, which bring dry and warm air from the Arabian Sea and suppress precipitation over these regions (Joseph et al., 2022). In addition, Hari et al., (2022) reported that a strong phase of Pacific meridional mode is leading a significant increase in heatwave over this regions. Overall, the spatial patterns in the dependence between precipitation and temperature during the ISM season are influenced by a complex interplay of local and large-scale circulation patterns, land-sea contrasts, SST anomalies, and other climatic factors. We obtain very similar results using the BIMD (Fig. S5) and APHRODITE (Fig. S6) datasets. The robustness of the results across different datasets suggests that the observed patterns are not sensitive to different data sources. These findings have implications for understanding the influence of negative P-T dependence on the likelihood of CDHE occurrence its variability.

Using the marginal distributions, we obtain the best-fit family by means of the maximum likelihood estimation (Fig. 3e-h). During June, the Frank family (no tail dependence) is the best fit for 60% of the grid points, while 25% show upper tail dependence (Joe family) and almost 15% show lower tail dependence (Clayton family) (Fig. S7). August shows very similar fractions as June. For July and September, the fraction of grid cells where the Frank family is preferred is clearly lower with around 40%, while the fractions of upper or lower tail dependence are much higher compared to June and August. There is a slight tendency to form spatial patterns, but these patterns are less well confined compared to the spatial patterns of P-T dependence and they change more strongly throughout the season. The grid cells with upper tail dependence are mostly concentrated in North-central India during June (Fig. 3e), in the North-western India during July (Fig. 3f), and scattered across North-central India and South-central India

during August (Fig. 3g) and September (Fig. 3h). Again, we obtain similar results using the BIMD (Fig. S5) and APHRODITE (Fig. S6) datasets revealing no sensitivity of the fitted copula to the different data sources.

Using the best-fit family, we obtain the LMF, i.e. the ratio of CDHE likelihood to the independent case. The spatial patterns of dependence and best-fit family translate into spatial patterns of LMF (Fig. 3i-l), hence both the strength of dependence and type of dependence are important. LMF ranges from 0.1 to 4.2 (Fig. 4). For example, LMF > 3 means that a 25-year CDHE in the independent case ($u \leq 0.2 \cap v > 0.8$) occurs on average every 8 years due to the P-T dependence. Regions with relatively high LMF values of around 3 are found over North-central India in June (Fig. 3i), over North-western parts in July (Fig. 3j), over South-central in August (Fig. 3k), and over Western India and South-central India in September (Fig. 3l). Hence, these regions have a high frequency of CDHE.

This spatial variation can be linked to the negative P-T dependence during JJAS (Fig. 3a-d). Precipitation and temperature have a negative association because the quantity of moisture that the air can store increases with temperature. Accordingly, as the temperature rises, the air can carry more water vapor and is less likely to saturate, which prevents precipitation from occurring. In contrast, if the temperature drops, the air becomes more likely to saturate, increasing the likelihood of precipitation (Trenberth et al., 2014; Trenberth and Shea, 2005). Another crucial factor to consider is the type of dependence exhibited in different regions. For example, in July, the North-Western and Western regions of India display different dependence patterns (Fig. 3b) and likelihoods (Fig. 3j) of CDHE occurrence. This variation is due to the copula type that best fits the dependence structure in each region (Fig. 3f). Upper tail dependence is evident in these regions, which amplifies the likelihood of CDHE occurrence. Even regions with moderate negative correlation can have a higher probability of CDHE when upper tail dependence is present (See Fig. 2, Fig. S8). The negative P-T dependence is primarily driven by the feedback between soil moisture and temperature, as discussed in the introduction and previous studies (Hao et al., 2022; Miralles et al., 2019; Zhang et al., 2021). This feedback mechanism is a major contributor to CDHE, and we will explore the hypothesis that soil moisture-temperature coupling is a key factor in the following section.

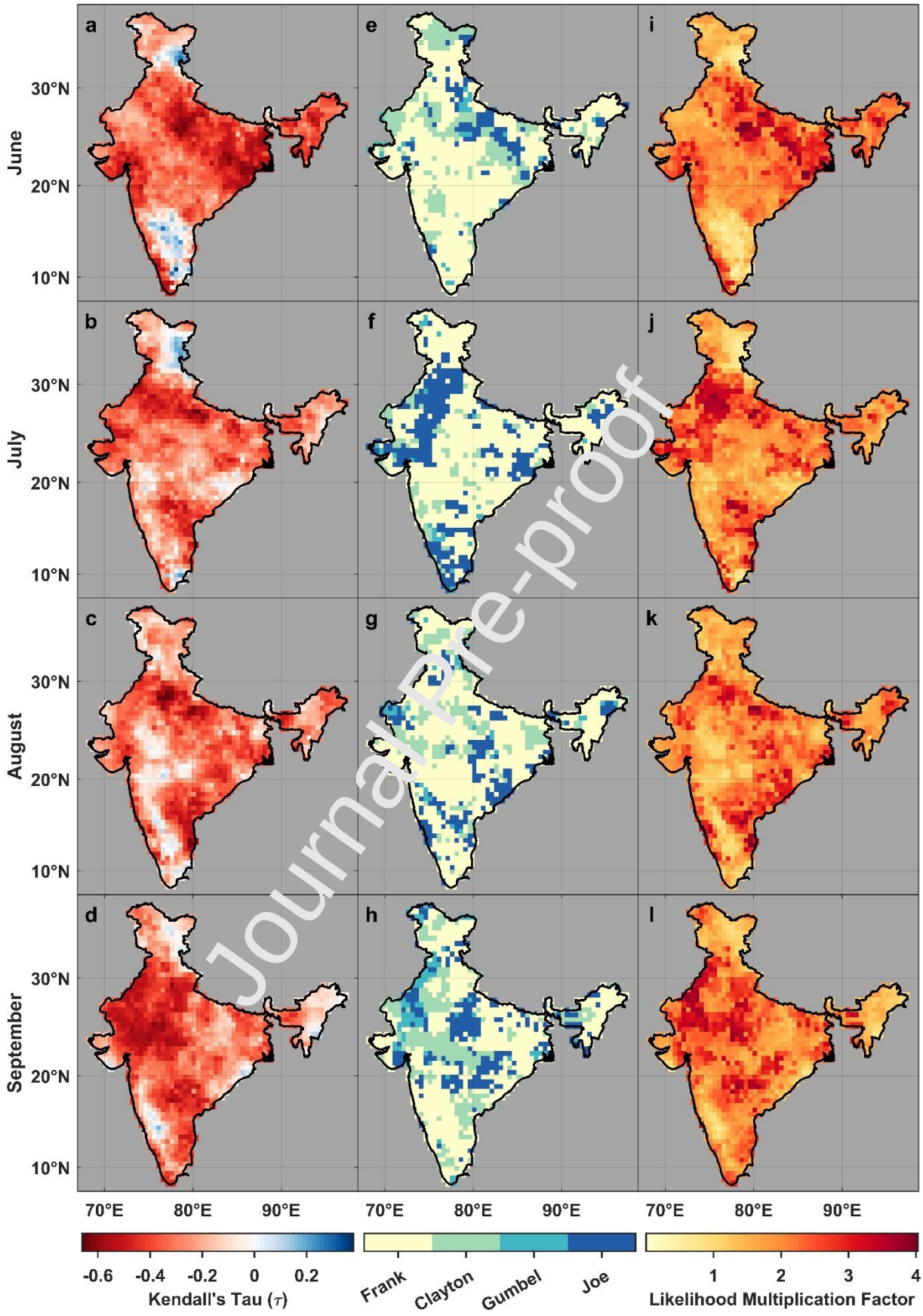

Figure 3: Kendall's Tau (τ) between monthly total precipitation and mean temperature during a) June, b) July, c) August, and d) September for 1961 to 1990. (e-h) Best-fit copula family (based on BIC) modelling the marginal cumulative distribution functions of precipitation and temperature and (i-l) Likelihood multiplication factor derived from respectively family.

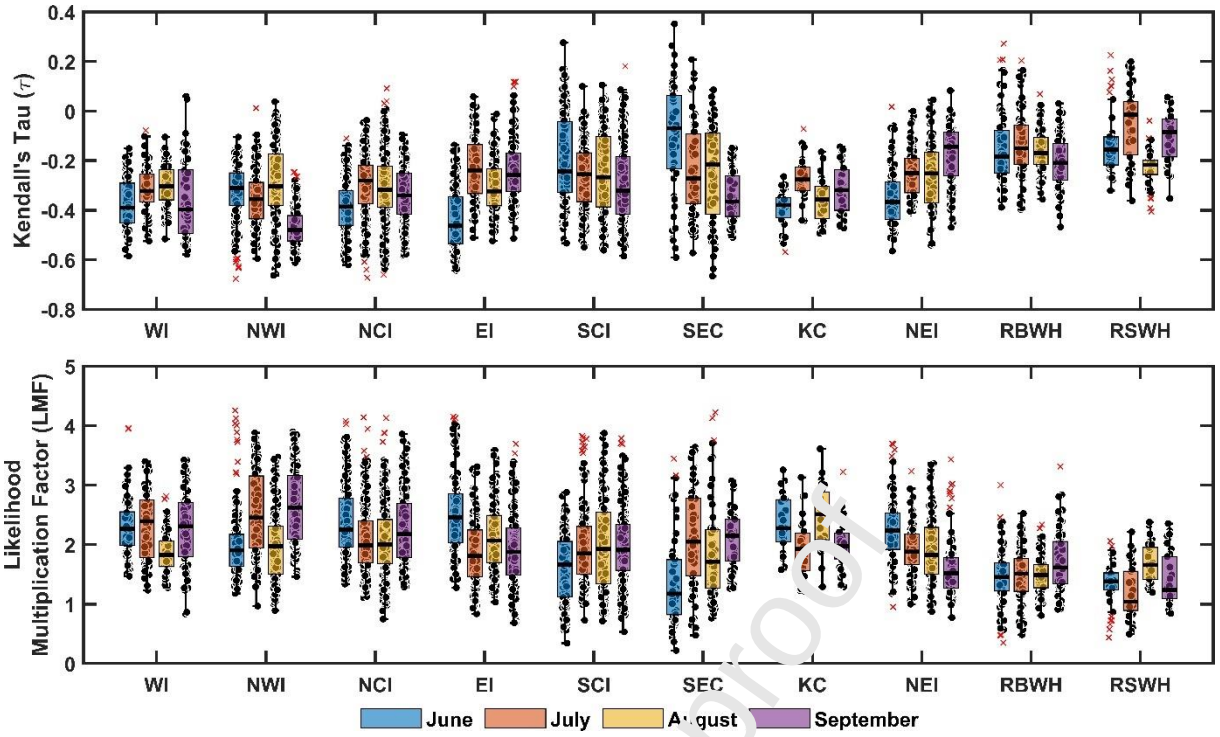

Figure 4: Boxplots of Kendall's Tau (top panel) and LMF (bottom panel) of sub-regions during June, July, August and September. The horizontal line shows the median, the box represents the IQR range, whiskers denote the 5th and 95th percentiles and points beyond the whiskers are outliers.

3.3 Disentangling the Role of Soil Moisture-Temperature Coupling on CDHE

Our results highlight that the occurrence of CDHE during ISM has a strong spatial diversity. We hypothesize that this variation is mainly caused by differences in land-atmospheric feedback. Therefore, to disentangle the role of soil moisture-temperature (SM-T) coupling on CDHEs across the sub-regions, we calculate the (instantaneous) precursor coincidence rate (Fig. 5a-d) and conditional precursor coincidence rate (Fig. 5e-h). For each grid point, we compute the 20th percentile for precipitation and soil moisture, and the 80th percentile for temperature given the monthly climatology for 1961-1990. Using these event time series, we apply event coincidence analysis to complement the copula approach. Specifically, we explore whether the spatial patterns between these two approaches match. P_{cr} quantifies to which extent hot extremes occur at the same time as dry extremes. Fig. 5a-d shows the dry and hot extremes instantaneous coincidence rate at a 0.05 significance level during the ISM across India from 1961 to 1990. Grids points with $P_{cr} > 0.60$ (60% of hot extremes occur simultaneously with dry extremes) are found across North-central and Eastern India in June (Fig. 5a), over North-western India and South-central India in July (Fig. 5b), over North-central India and South-central India in August (Fig. 5c), and over Western, North-central, and South-central India in September (Fig. 5d). The spatial variation of P_{cr} is in line with the spatial variation of the negative P-T dependence (Fig. 3a-d) and highlights the effect of the negative association between precipitation and temperature on CDHE likelihood.

We use the (instantaneous) conditional precursor coincidence rate and test the hypothesis of whether low soil moisture pre-conditioned by dry extremes triggers hot

extremes or not. Fig. 5e-h illustrates the spatial variation of CP_{cr} between hot extremes, low soil moisture and dry extremes. The spatial variation of CP_{cr} follows closely the spatial variation of P_{cr} (Fig. 5a-d). This correspondence suggests that precipitation deficits result in the depletion of soil moisture which in turn aggravates high temperatures, leading to the simultaneous occurrence of CDHE.

According to Rajeev et al., (2022), dry weather conditions can cause a rise in local temperatures over the Northwest and Southern regions of India during the ISM season, as soil moisture deficits lead to the conversion of incoming shortwave radiation into sensible heat. The study identified that the relationship between soil moisture and temperature is a key factor contributing to the occurrence of CDHEs in North-western and South-Central India. However, Mishra et al., (2022) reviewed that due to the ISM's intra-seasonal variability, it is challenging to assess CDHEs for the entire season. Therefore, the focus of this study was on the monthly timescale. The results indicated that CDHEs in North-western and South-central India are more likely to occur between July and September, excluding June. Karmakar and Misra, (2019) reported that June marks the onset of the ISM season, and the area experiences a significant rise in precipitation and a drop in temperatures during this time. The increase in precipitation aids in replenishing soil moisture, reducing the probability of soil moisture deficits, which are a significant driver of CDHEs. Additionally, Ambika and Mishra, (2019) reported that irrigation has made this region less vulnerable to CDHEs. Therefore, this region is more susceptible to water stress during the mature and withdrawal stages of the season than during the onset of ISM.

The study also identified North-central India as a hotspot for CDHEs, with a high likelihood of occurrence between the onset of the monsoon (June) and the conclusion of the mature phase (August). This finding is consistent with a previous study by Ganeshi et al., (2020), which found a strong relationship between soil moisture and temperature in North-central India. Rajeev et al., (2016) suggested that atmospheric blocking over the North Atlantic leads to hot extremes over North-central India, while anomalous cooling in the tropical West Pacific is responsible for hot extremes over South-central India. In both regions, low soil moisture levels resulting from dry conditions can explain the occurrence of CDHEs with a probability of 0.5-0.6.

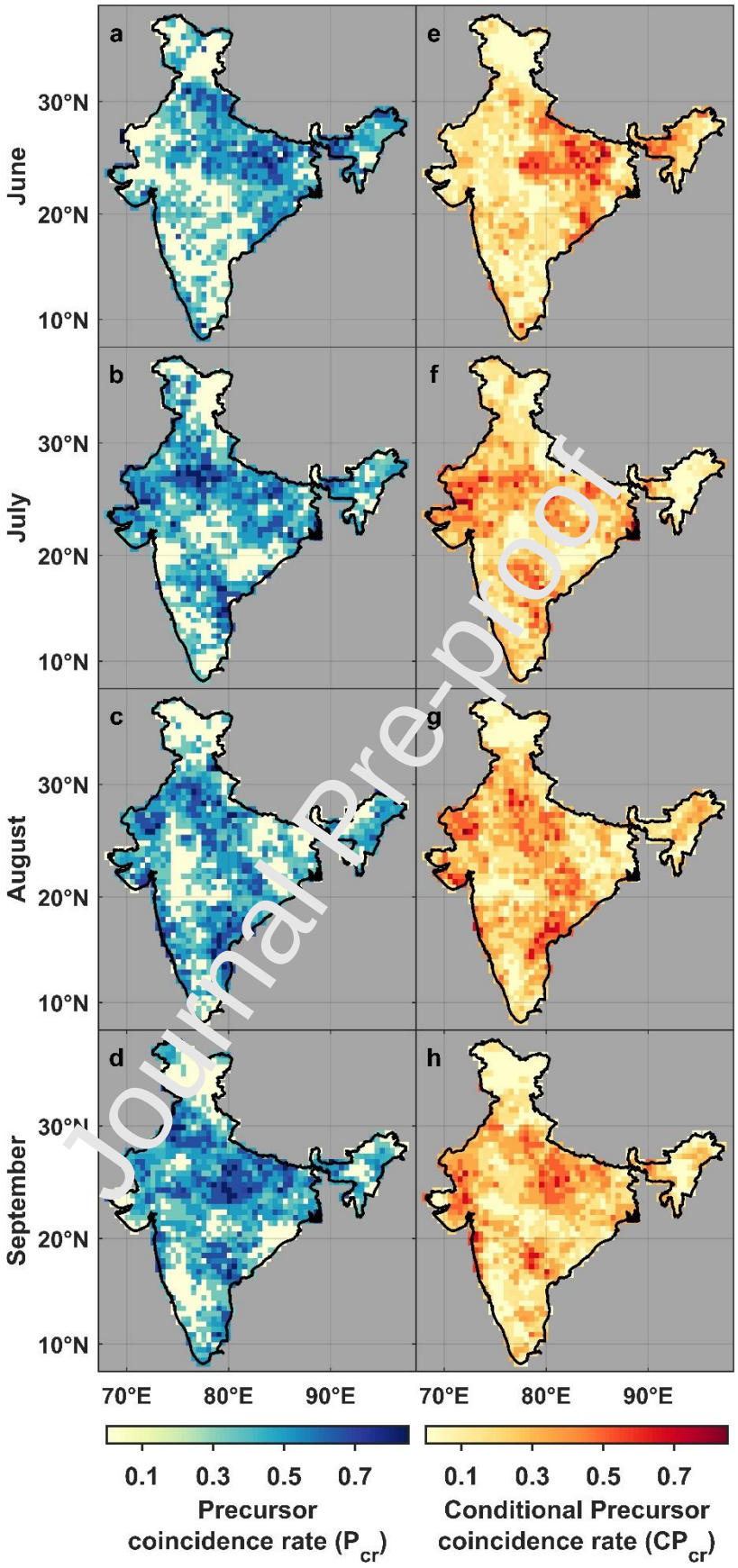

Figure 5: Precursor coincidence rate (P_{cr}) between hot and dry extremes during a) June, b) July, c) August, and d) September for 1961 to 1990. (e-h) shows the conditional precursor coincidence rate (CP_{cr}) between hot extremes, low soil moisture and dry extremes. The colorbar represents the variation in the coincidence rate at the 95% confidence level.

3.4 Temporal evolution of CDHE likelihood

In India during the past decades, an increased frequency of CDHEs with widespread spatial extent has been observed, particularly in North-central India and the South-eastern coastlines (Guntu and Agarwal, 2021; Mishra et al., 2020b; Rajeev et al., 2022; Sharma and Mujumdar, 2017). To understand the evolving nature of P-T dependence over time and its impact on LMF, we compute the Kendall rank correlation and LMF for each 30-year period starting from the baseline period 1961-1990 with a 1-year moving window. For each grid cell, we thus obtain time series of length 25 (1961-1990, 1962-1991, …, 1985-2014) for Kendall's tau and LMF, respectively. We determine their temporal changes by calculating Sen's slope (Sen, 1968) and test for trends at the 0.05 significance level using the modified Mann-Kendall test (Hamed and Ramachandra Rao, 1998).

As there is a direct relationship exists between P-T dependence and LMF, an enhanced negative P-T dependence leads to an increase in LMF and vice versa. Figure. 6 maps the trends in P-T dependence and in LMF across India. Further, it exemplarily illustrates their time variations for four selected grid points. These grid points are randomly selected to show the significant increase in the negative correlation between precipitation and temperature during JJAS. Enhanced negative P-T dependence is seen over parts of South-central India and South-eastern coastlines during June (Fig. 6a), which contributes to a more frequent CDHE (Fig. 6e). LMF has doubled in the last 30-year period compared to the baseline period (Fig. 6i). Guntu & Agarwal (2021) reported that no discernible change in precipitation is observed in these regions. The rise in temperature over this region is the primary factor contributing to the LMF increase. Negative P-T dependence in July (Fig. 6b) has mainly increased over parts of North-central India, Eastern India, Konkan coast and North-eastern India, leading to an increase in CDHE likelihood (Fig. 6f) and a tripling of LMF during 1961-2014 for the grid point over North-central India (Fig. 6j). Mondal et al. (2015) reported that in July precipitation is decreasing and temperature is rising. Therefore, an increase in LMF in this region is attributable to changes in temperature and precipitation patterns.

An increase in CDHE likelihood is observed over parts of North-western and North-central India in August (Fig. 6g) attributable to increased negative P-T dependence (Fig. 6c). For instance, a significant trend of P-T dependence with a slope of -0.20/decade has led to an increase of LMF slope of 1.0/decade during 1961-2014 for the grid point in North-western India (Fig. 6k). Previous studies (Deshpande et al., 2016; Guntu et al., 2020; Kulkarni et al., 2020; Taxak et al., 2014) concluded that precipitation over these regions is decreasing, Roxy et al. (2017) suggested that this effect is a consequence of a large-scale decline in the transport of moisture from the Arabian Sea down the west coast onto the mainland, which is referred to as the weakening of monsoon circulation due to the eastern equatorial Indian Ocean's rapid warming. Due to an increase in aerosol content, Bollasina et al., (2011) found that the heat gradient between the north and south Indian oceans (which is responsible for the tropical circulation along the zonal component) is decreasing. According to Naidu et al., (2015), the number of low-pressure systems traveling to these regions has decreased due to a decrease in the strength of the

tropical easterly jet stream. Likewise, Sandeep et al. (2018) found that the poleward shift in ISM synoptic activity due to the warming climate is responsible for the reduction. The average temperature in these regions is also increasing significantly. As a result, decreasing precipitation and rising temperature have been identified as major drivers of the increased likelihood of CDHE.

Strengthened negative P-T dependence is shown across parts of South-central India, Southern-eastern coastlines and North-eastern India in September (Fig. 6d) resulting in increased CDHE likelihood (Fig. 6h). For the grid point in South-central India (Fig. 6l), a three-fold rise in LMF is observed resulting from the strengthened negative dependence from -0.09 for the period 1961-1990 to –0.52 for 1985-2014. The results suggest that the negative P-T dependence has increased, indicating a higher chance of CDHE occurrence in these regions. Saha et al. (2022) observed a widespread increase in warm nights and a drop in precipitation intensity over North-Eastern India. They concluded that changes in the Atlantic meridional mode alter the dynamics of weather extremes in this region. Barman & Gokhale (2022) employed a Weather Research and Forecasting (WRF) model coupled with chemistry and established that aerosols are the reason for the decrease in rainfall activity. Using the WRF model, Lal et al. (2021) found that extensive changes in land use and land cover have caused temperature to rise $\sim 0.4^{o}C$ from 2002 to 2015. Similarly, Gogoi et al. (2019) indicated that LULC-induced warming is responsible for almost 25% of the mean temperature increase since 2001 in Eastern India. As a result, the increase in LMF in these regions can be attributed to both decreasing precipitation and rising temperature.

Maps (Fig. 6e-h) also show some regions without changes and some with decreasing LMF values. The overall pattern of changes in the likelihood of CDHE in India is shown by the boxplots of changes in P-T dependence (Fig. 6m) and LMF (Fig. 6n) over all grid points during JJAS. According to the distribution of LMF/decade for June (Fig. 6n), 50% of the grid cells have positive trends, 25% have negative trends, and 25% have no trends. As much of the world's temperature continues to rise, trends in precipitation affect the likelihood of CDHE in the future (Bevacqua et al., 2022). We identified a negative association between June's total precipitation and mean temperature waning over parts of North-western India and Konkan coast for June (Fig. 6e). According to a previous study by Subash & Sikka (2014), the precipitation in June in this region shows a positive trend. In July, > 70% of the grid cells exhibited an enhanced negative P-T dependence, while the remaining 30% exhibited a declining negative correlation (Fig. 6m). However, a positive trend in LMF is visible only in more than 50% of the grid cells (Fig. 6n). The majority of grid cells with a decrease in LMF are found in Western India and South-central India, which is in line with rising precipitation patterns based on a long-term dataset (Guhathakurta et al., 2015).

August and September see an equal distribution of changes in positive and negative trends in LMF (Fig. 6n). In August, the decrease in negative P-T dependence is seen across parts of South-central India and Konkan coast (Fig. 6c). According to Kumar et al., (2010) , August precipitation showed statistically significant increasing trends, implying

that changing precipitation is the recent major driver to the decreased likelihood of CDHE. In September (Fig. 6d), an increase in LMF is found over a few grid cells in North-western India despite a decline in the negative P-T dependence. To illustrate this counterintuitive result, the temporal pattern of Kendall's tau slope, best-fit family and of the LMF slope is shown in Fig. S8 for each 30-year period starting from the baseline period with a 1-year moving window for September over the grid point $(76.75^0E, 24.25^0N)$ of North-western India. Despite a decline in the negative association between precipitation and temperature (Fig. S8a), a shift in the distribution type (Fig. S8b) led to an increase in LMF in the recent decades (Fig. S8c). Once again, we obtain similar results using the BIMD dataset (Fig. S9), which reveals the robustness of the trends to a different data source. Previous research (Guntu and Agarwal, 2021; Mishra et al., 2020b; Rajeev et al., 2022; Sharma and Mujumdar, 2017) reported the rising trend of CDHEs, but the intra-seasonal spatiotemporal variability in the likelihood of CDHE and the hypothesis of soil moisture-temperature coupling was never reported, highlighting the novel contribution of our study.

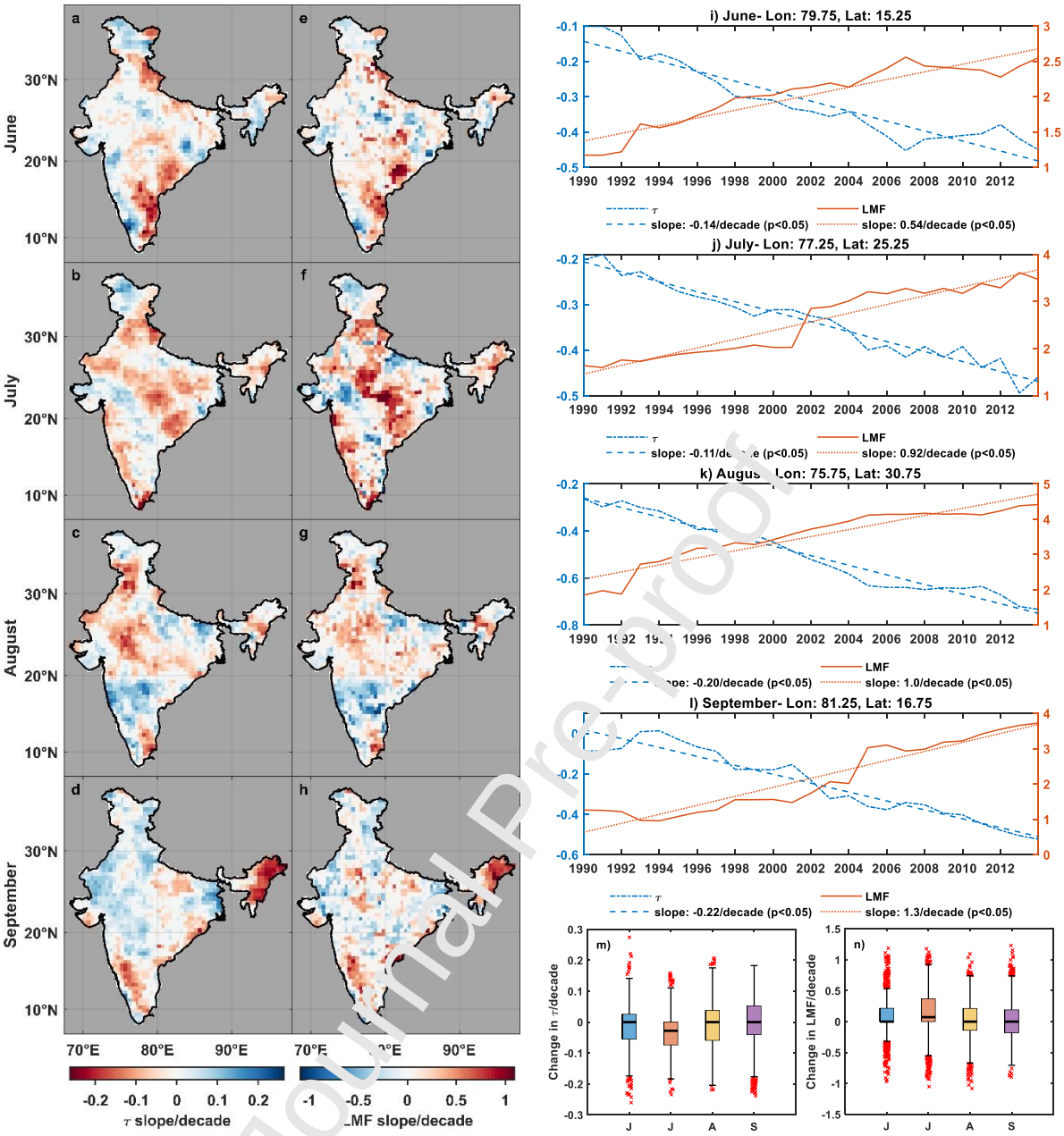

Figure 6: Spatial patterns of trend slope of Kendall's tau (a-d) and of the Likelihood Multiplication Factor (e-h) for each 30-year period starting from the baseline period 1961-1990 with 1-year moving window for June, July, August and September (JJAS). For selected grid cells, trends of P-T dependence (blue) and LMF (red) are shown in (i-l). Trends are shown for 30-year periods (blue – dashed-dotted; red – solid) and for the entire period (blue – dashed; red – dotted). Also, boxplots of change in Kendall's tau per decade (m) and change in LMF/decade (n) over all grid points are showed for JJAS. The box represents the range between the first and third quartile, horizontal black line within the box represents the median, and the outermost markers on either side of the box are the minimum and maximum values.

4 Conclusions

We investigated the likelihood, spatial diversity and responsible mechanisms of Compound Dry and Hot Extremes (CDHE) occurrence during the Indian summer monsoon across India. Our results highlighted strong intra-seasonal and spatiotemporal variability in the likelihood of CDHE. For instance, we found a high likelihood of CDHE over North-Central India and Eastern India for June, Western India, North-Western, North-central India and South-central India for July, North-Central India and Konkan coast for August, Western India, North-Western India and South-central India for September. Regions with upper tail dependence primarily concentrated in North-central

India for June, Western India and North-western India for July, and were scattered across North-central India and South-central India for August and September. Event coincidence analysis (ECA) reveals that low soil moisture pre-conditioned by dry extremes is responsible for 55% to 65% of CDHE occurrence. However, ECA is a statistical method used to investigate the potential relationships between two or more time series data. ECA can identify whether certain events in one series tend to coincide with certain events in another series more often than expected by chance. Understanding the physical mechanisms of soil moisture-temperature coupling requires a comprehensive understanding of the underlying physical processes involved, such as energy and water balance in the land-atmosphere system. ECA can help to identify potential relationships between soil moisture and temperature, but it is not a substitute for a physical understanding of the mechanisms at play. The temporal evolution of the likelihood of CDHE occurrence confirms a 2- to 3-fold rise in CDHE from 1961 to 2014 for several regions across India. Further research can incorporate the consequences of CDHE to produce more meaningful risk assessments. This research serves as a useful foundation for assessing the likelihood of CDHE occurrence and developing adaptation strategies in India amidst global warming.

Data Availability Statement

We thank all the following agencies for archiving and making data accessible. University of Delaware: https://psl.noaa.gov/data/gridded/data.UDel_AirT_Precip.html (V5.01 accessed on December 2021); CPC Soil Moisture: https://psl.noaa.gov/data/gridded/data.cpcsoil.html (accessed on August, 2022); Bias-corrected IMD: https://doi.org/10.5281/zenodo.3987736 (accessed on August, 2021); APHRODITE: http://aphrodite.st.hirosaki-u.ac.jp/download/ (V1101 accessed on October, 2022).

Declaration of Conflict of Interest:

The authors declare no conflicts of interest relevant to this study.

Acknowledgments

RKG would like to express sincere gratitude for the financial support received from the Prime Minister's Research Fellowship (PM-31-22-695-414), Government of India and DAAD, Germany (Ref No: 91800544). AA would like to acknowledge the joint funding support from the University Grant Commission (UGC) and DAAD under the Indo-German Partnership in Higher Education (IGP) framework at the IIT Roorkee. We also extend our thanks to the reviewers for their valuable feedback, which contributed to improving the quality of the manuscript.

Author Contributions:

Conceptualization	: Ravi Kumar Guntu, Bruno Merz, Ankit Agarwal
Data curation	: Ravi Kumar Guntu
Formal analysis	: Ravi Kumar Guntu
Funding acquisition	: Ravi Kumar Guntu, Ankit Agarwal
Investigation	: Ravi Kumar Guntu
Methodology	: Ravi Kumar Guntu, Bruno Merz, Ankit Agarwal

Project Administration	: Ankit Agarwal
Software	: Ravi Kumar Guntu
Supervision	: Bruno Merz, Ankit Agarwal
Validation	: Ravi Kumar Guntu, Bruno Merz
Writing – original draft	: Ravi Kumar Guntu
Writing – review & editing	: Bruno Merz, Ankit Agarwal

Appendix A

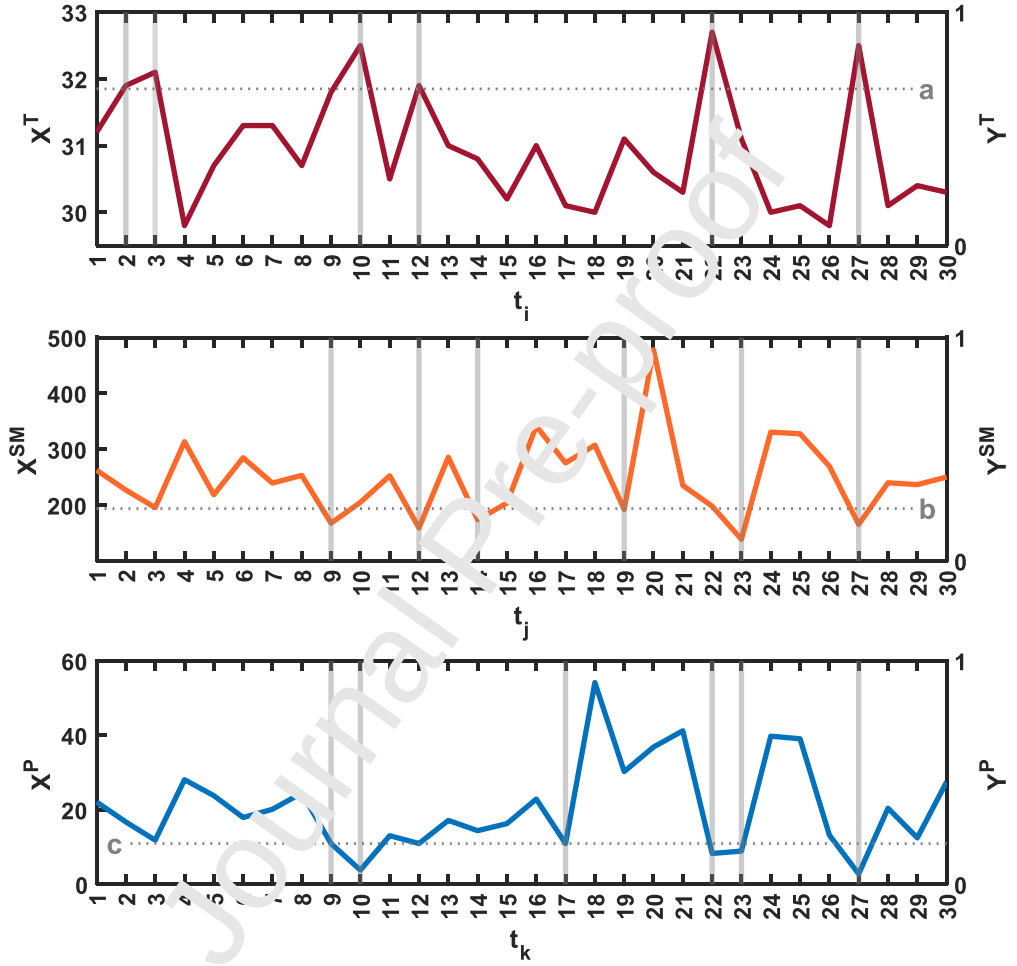

Figure A1: Illustration of time series of the average temperature (X^T), average soil moisture (X^{SM}) and total precipitation (X^P) at timesteps t_i, t_j and t_k, respectively for a specific month in one climate normal. The vertical and horizontal lines are included to visualize the event (Y^T, Y^{SM}, Y^P) and the threshold (a, b, c) used to define it.

References

Aihaiti, A., Jiang, Z., Zhu, L., Li, W., You, Q., 2021. Risk changes of compound temperature and precipitation extremes in China under 1.5 °C and 2 °C global warming. Atmospheric Research 264, 105838. https://doi.org/10.1016/j.atmosres.2021.105838

Ambika, A.K., Mishra, V., 2019. Observational Evidence of Irrigation Influence on Vegetation Health and Land Surface Temperature in India. Geophysical Research Letters 46, 13441–13451. https://doi.org/10.1029/2019GL084367

Barman, N., Gokhale, S., 2022. Aerosol influence on the pre-monsoon rainfall mechanisms over North-East India: A WRF-Chem study. Atmospheric Research 268, 106002. https://doi.org/10.1016/j.atmosres.2021.106002

Berg, A., Findell, K., Lintner, B., Giannini, A., Seneviratne, S.I., van den Hurk, B., Lorenz, R., Pitman, A., Hagemann, S., Meier, A., Cheruy, F., Ducharne, A., Malyshev, S., Milly, P.C.D., 2016. Land–atmosphere feedbacks amplify aridity increase over land under global warming. Nature Clim Change 6, 869–874. https://doi.org/10.1038/nclimate3029

Berg, A., Lintner, B.R., Findell, K., Seneviratne, S.I., van den Hurk, B., Ducharne, A., Chéruy, F., Hagemann, S., Lawrence, D.M., Malyshev, S., Meier, A., Gentine, P., 2015. Interannual Coupling between Summertime Surface Temperature and Precipitation over Land: Processes and Implications for Climate Change*. Journal of Climate 28, 1308–1328. https://doi.org/10.1175/JCLI-D-14-00324.1

Bevacqua, E., Zappa, G., Lehner, F., Zscheischler, J., 2022. Precipitation trends determine future occurrences of compound hot–dry events. Nat. Clim. Chang. 12, 350–355. https://doi.org/10.1038/s41558-022-01309-5

Bhatla, R., Singh, A.K., Mandal, B., Ghosh, S., Pandey, S.N., Sarkar, A., 2016. Influence of North Atlantic Oscillation on Indian Summer Monsoon Rainfall in Relation to Quasi-Binneal Oscillation. Pure Appl. Geophys. 173, 2959–2970. https://doi.org/10.1007/s00024-016-1306-z

Bollasina, M.A., Ming, Y., Ramaswamy, V., 2011. Anthropogenic Aerosols and the Weakening of the South Asian Summer Monsoon. Science 334, 502–505. https://doi.org/10.1126/science.1204994

Das, J., Manikanta, V., Umamahesh, N.V., 2022. Population exposure to compound extreme events in India under different emission and population scenarios. Science of The Total Environment 806, 150424. https://doi.org/10.1016/j.scitotenv.2021.150424

Dash, S., Maity, R., 2023. Unfolding unique features of precipitation-temperature scaling across India. Atmospheric Research 284, 106601. https://doi.org/10.1016/j.atmosres.2022.106601

Deshpande, N.R., Kothawale, D.R., Kulkarni, A., 2016. Changes in climate extremes over major river basins of India: CLIMATE EXTREMES IN INDIA. Int. J. Climatol. 36, 4548–4559. https://doi.org/10.1002/joc.4651

Donges, J.F., Schleussner, C.-F., Siegmund, J.F., Donner, R.V., 2016. Event coincidence analysis for quantifying statistical interrelationships between event time series: On the role of flood events as triggers of epidemic outbreaks. Eur. Phys. J. Spec. Top. 225, 471–487. https://doi.org/10.1140/epjst/e2015-50233-y

Ganeshi, N.G., Mujumdar, M., Krishnan, R., Goswami, M., 2020. Understanding the linkage between soil moisture variability and temperature extremes over the Indian region. Journal of Hydrology 589, 125183. https://doi.org/10.1016/j.jhydrol.2020.125183

Ganguli, P., 2023. Amplified risk of compound heat stress-dry spells in Urban India. Clim Dyn 60, 1061–1078. https://doi.org/10.1007/s00382-022-06324-y

Ganguli, P., Merz, B., 2019. Trends in Compound Flooding in Northwestern Europe During 1901–2014. Geophys. Res. Lett. 46, 10810–10820. https://doi.org/10.1029/2019GL084220

Genest, C., Favre, A.-C., 2007. Everything You Always Wanted to Know about Copula Modeling but Were Afraid to Ask. J. Hydrol. Eng. 12, 347–368. https://doi.org/10.1061/(ASCE)1084-0699(2007)12:4(347)

Gogoi, P.P., Vinoj, V., Swain, D., Roberts, G., Dash, J., Tripathy, S., 2019. Land use and land cover change effect on surface temperature over Eastern India. Sci Rep 9, 8859. https://doi.org/10.1038/s41598-019-45213-z

Guhathakurta, P., Rajeevan, M., Sikka, D.R., Tyagi, A., 2015. Observed changes in southwest monsoon rainfall over India during 1901-2011: TREND IN SOUTHWEST MONSOON RAINFALL OVER INDIA. Int. J. Climatol 35, 1881–1898. https://doi.org/10.1002/joc.4095

Guntu, R.K., Agarwal, A., 2021. Disentangling increasing compound extremes at regional scale during Indian summer monsoon. Sci Rep 11, 16447. https://doi.org/10.1038/s41598-021-95775-0

Guntu, R.K., Maheswaran, R., Agarwal, A., Singh, V.P., 2020. Accounting for temporal variability for improved precipitation regionalization based on self-organizing map coupled with information theory. Journal of Hydrology 590, 125236. https://doi.org/10.1016/j.jhydrol.2020.125236

Gupta, V., Kumar Jain, M., Singh, V.P., 2020. Multivariate Modeling of Projected Drought Frequency and Hazard over India. J. Hydrol. Eng. 25, 04020003. https://doi.org/10.1061/(ASCE)HE.1943-5584.0001893

Hamed, K.H., Ramachandra Rao, A., 1998. A modified Mann-Kendall trend test for autocorrelated data. Journal of Hydrology 204, 182–196. https://doi.org/10.1016/S0022-1694(97)00125-X

Hao, Z., AghaKouchak, A., 2014. A Nonparametric Multivariate Multi-Index Drought Monitoring Framework. Journal of Hydrometeorology 15, 89–101. https://doi.org/10.1175/JHM-D-12-0160.1

Hao, Z., Hao, F., Xia, Y., Feng, S., Sun, C., Zhang, X., Fu, Y., Hao, Y., Zhang, Y., Meng, Y., 2022. Compound droughts and hot extremes: Characteristics, drivers, changes, and impacts. Earth-Science Reviews 235, 104241. https://doi.org/10.1016/j.earscirev.2022.104241

Hao, Z., Singh, V.P., 2020. Compound Events under Global Warming: A Dependence Perspective. J. Hydrol. Eng. 25, 03120001. https://doi.org/10.1061/(ASCE)HE.1943-5584.0001991

Hari, V., Ghosh, S., Zhang, W., Kumar, R., 2022. Strong influence of north Pacific Ocean variability on Indian summer heatwaves. Nat Commun 13, 5349. https://doi.org/10.1038/s41467-022-32942-5

Hrudya, P.H., Varikoden, H., Vishnu, R., 2021. A review on the Indian summer monsoon rainfall, variability and its association with ENSO and IOD. Meteorol Atmos Phys 133, 1–14. https://doi.org/10.1007/s00703-020-00734-5

Jha, R., Mondal, A., Devanand, A., Roxy, M.K., Ghosh, S., 2022. Limited influence of irrigation on pre-monsoon heat stress in the Indo-Gangetic Plain. Nat Commun 13, 4275. https://doi.org/10.1038/s41467-022-31962-5

Joseph, S., Sahai, A.K., Shabu, H., Chattopadhyay, R., Kaur, M., 2022. Recent changes in the spatio-temporal characteristics of monsoon intraseasonal oscillations. Theor Appl Climatol 147, 251–264. https://doi.org/10.1007/s00704-021-03830-7

Kanda, N., Negi, H.S., Rishi, M.S., Kumar, A., 2020. Performance of various gridded temperature and precipitation datasets over Northwest Himalayan Region. Environ. Res. Commun. 2, 085002. https://doi.org/10.1088/2515-7620/ab9991

Karmakar, N., Misra, V., 2019. The Relation of Intraseasonal Variations With Local Onset and Demise of the Indian Summer Monsoon. JGR Atmospheres 124, 2483–2506. https://doi.org/10.1029/2018JD029642

Kathayat, G., Sinha, A., Breitenbach, S.F.M., Tan, L., Spötl, C., Li, H., Dong, X., Zhang, H., Ning, Y., Allan, R.J., Damodaran, V., Edwards, R.L., Cheng, H., 2022. Protracted Indian monsoon droughts of the past millennium and their societal impacts. Proc. Natl. Acad. Sci. U.S.A. 119, e2207487119. https://doi.org/10.1073/pnas.2207487119

Kulkarni, A., Sabin, T.P., Chowdary, J.S., Rao, K.K., Priya, P., Gandhi, N., Bhaskar, P., Buri, V.K., Sabade, S.S., Pai, D.S., Ashok, K., Mitra, A.K., Niyogi, D., Rajeevan, M., 2020. Precipitation Changes in India, in: Krishnan, R., Sanjay, J., Gnanaseelan, C., Mujumdar, M., Kulkarni, A., Chakraborty, S. (Eds.), Assessment of Climate Change over the Indian Region. Springer Singapore, Singapore, pp. 47–72. https://doi.org/10.1007/978-981-15-4327-2_3

Kumar, V., Jain, S.K., Singh, Y., 2010. Analysis of long-term rainfall trends in India. Hydrological Sciences Journal 55, 484–496. https://doi.org/10.1080/02626667.2010.481373

Lal, P., Shekhar, A., Kumar, A., 2021. Quantifying Temperature and Precipitation Change Caused by Land Cover Change: A Case Study of India Using the WRF Model. Front. Environ. Sci. 9, 766328. https://doi.org/10.3389/fenvs.2021.766328

Mallya, G., Mishra, V., Niyogi, D., Tripathi, S., Govindaraju, R.S., 2016. Trends and variability of droughts over the Indian monsoon region. Weather and Climate Extremes 12, 43–68. https://doi.org/10.1016/j.wace.2016.01.002

Manoj, J.A., Guntu, R.K., Agarwal, A., 2022. Spatiotemporal Dependence of Soil Moisture and Precipitation over India. Journal of Hydrology 127898. https://doi.org/10.1016/j.jhydrol.2022.127898

Meng, Y., Hao, Z., Feng, S., Zhang, X., Hao, F., 2022. Increase in compound dry-warm and wet-warm events under global warming in CMIP6 models. Global and Planetary Change 210, 103773. https://doi.org/10.1016/j.gloplacha.2022.103773

Miralles, D.G., Gentine, P., Seneviratne, S.I., Teuling, A.J., 2019. Land-atmospheric feedbacks during droughts and heatwaves: state of the science and current challenges: Land feedbacks during droughts and heatwaves. Ann. N.Y. Acad. Sci. 1436, 19–35. https://doi.org/10.1111/nyas.13912

Mishra, V., Bhatia, U., Tiwari, A.D., 2020a. Bias-corrected climate projections for South Asia from Coupled Model Intercomparison Project-6. Sci Data 7, 338. https://doi.org/10.1038/s41597-020-00681-1

Mishra, V., Mujumdar, M., Mahto, S.S., 2022. Benchmark worst droughts during the summer monsoon in India. Phil. Trans. R. Soc. A. 380, 20210291. https://doi.org/10.1098/rsta.2021.0291

Mishra, V., Thirumalai, K., Singh, D., Aadhar, S., 2020b. Future exacerbation of hot and dry summer monsoon extremes in India. npj Clim Atmos Sci 3, 10. https://doi.org/10.1038/s41612-020-0113-5

Mondal, A., Khare, D., Kundu, S., 2015. Spatial and temporal analysis of rainfall and temperature trend of India. Theor Appl Climatol 122, 143–158. https://doi.org/10.1007/s00704-014-1283-z

Mukherjee, S., Mishra, A.K., Zscheischler, J., Entekhabi, D., 2023. Interaction between dry and hot extremes at a global scale using a cascade modeling framework. Nat Commun 14, 277. https://doi.org/10.1038/s41467-022-35748-7

Naidu, C.V., Dharma Raju, A., Satyanarayana, G.Ch., Vinay Kumar, P., Chiranjeevi, G., Suchitra, P., 2015. An observational evidence of decrease in Indian summer monsoon rainfall in the recent three decades of global warming era. Global and Planetary Change 127, 91–102. https://doi.org/10.1016/j.gloplacha.2015.01.010

Navale, A., Karthikeyan, L., 2023. Understanding Recycled Precipitation at Different Spatio-Temporal Scales Over India: An Eulerian Water Tagging Approach. Water Resources Research 59. https://doi.org/10.1029/2022WR032605

Nikoloulopoulos, A.K., Joe, H., Li, H., 2012. Vine copulas with asymmetric tail dependence and applications to financial return data. Computational Statistics & Data Analysis 56, 3659–3673. https://doi.org/10.1016/j.csda.2010.07.016

Osman, M., Zaitchik, B.F., Winstead, N.S., 2022. Cascading Drought-Heat Dynamics During the 2021 Southwest United States Heatwave. Geophysical Research Letters 49. https://doi.org/10.1029/2022GL099265

Oza, H., Padhya, V., Gangaiv, A., Deshpande, R.D., 2022. Investigating hydrometeorology of the Western Himalayas: Insights from stable isotopes of water and meteorological parameters. Atmospheric Research 268, 105997. https://doi.org/10.1016/j.atmosres.2021.105997

Rajeev, A., Mahto, S.S., Mishra, V., 2022. Climate warming and summer monsoon breaks drive compound dry and hot extremes in India. iScience 25, 105377. https://doi.org/10.1016/j.isci.2022.105377

Ratnam, J.V., Behera, S.K., Ratna, S.B., Rajeevan, M., Yamagata, T., 2016. Anatomy of Indian heatwaves. Sci Rep 6, 24395. https://doi.org/10.1038/srep24395

Rawat, S., Ganapathy, A., Agarwal, A., 2022. Drought characterization over Indian sub-continent using GRACE-based indices. Sci Rep 12, 15432. https://doi.org/10.1038/s41598-022-18511-2

Raymond, C., Horton, R.M., Zscheischler, J., Martius, O., AghaKouchak, A., Balch, J., Bowen, S.G., Camargo, S.J., Hess, J., Kornhuber, K., Oppenheimer, M., Ruane, A.C., Wahl, T., White, K., 2020. Understanding and managing connected extreme events. Nat. Clim. Chang. 10, 611–621. https://doi.org/10.1038/s41558-020-0790-4

Ridder, N.N., Pitman, A.J., Ukkola, A.M., 2021. Do CMIP6 Climate Models Simulate Global or Regional Compound Events Skillfully? Geophysical Research Letters 48. https://doi.org/10.1029/2020GL091152

Ridder, N.N., Pitman, A.J., Westra, S., Ukkola, A., Do, H.X., Bador, M., Hirsch, A.L., Evans, J.P., Di Luca, A., Zscheischler, J., 2020. Global hotspots for the occurrence of compound events. Nat Commun 11, 5956. https://doi.org/10.1038/s41467-020-19639-3

Roxy, M.K., Ghosh, S., Pathak, A., Athulya, R., Mujumdar, M., Murtugudde, R., Terray, P., Rajeevan, M., 2017. A threefold rise in widespread extreme rain events over central India. Nat Commun 8, 708. https://doi.org/10.1038/s41467-017-00744-9

Saha, S., Chakraborty, Debasish, Hazarika, S., Shakuntala, I., Das, B., Chhabra, A., Sadhu, S., Chakraborty, Debashis, Mukherjee, J., Singson, L., Mishra, V.K., 2022. Spatiotemporal variability of weather extremes over eastern India: evidences of ascertained long-term trend persistence and effective global climate controls. Theor Appl Climatol 148, 643–659. https://doi.org/10.1007/s00704-022-03949-1

Salvadori, G., De Michele, C., 2010. Multivariate multiparameter extreme value models and return periods: A copula approach. Water Resour. Res. 46, 2009WR009040. https://doi.org/10.1029/2009WR009040

Sandeep, S., Ajayamohan, R.S., Boos, W.R., Sabin, T.P., Praveen, V., 2018. Decline and poleward shift in Indian summer monsoon synoptic activity in a warming climate. Proc. Natl. Acad. Sci. U.S.A. 115, 2681–2686. https://doi.org/10.1073/pnas.1709021115

Sankar, S., Vijaykumar, P., Abhilash, S., Mohanakumar, K., 2021. Influence of the strongest positive Indian Ocean Dipole and an El Niño Modoki event on the 2019 Indian summer monsoon. Dynamics of Atmospheres and Oceans 95, 101235. https://doi.org/10.1016/j.dynatmoce.2021.101235

Schepsmeier, U., Stoeber, J., Brechmann, E.C., Graeler, B., Nagler, T., Erhardt, T., Almeida, C., Min, A., Czado, C., Hofmann, M., others, 2015. Package 'vinecopula.' R package version 2.

Schumacher, D.L., Keune, J., Dirmeyer, P., Miralles, D.G., 2022. Drought self-propagation in drylands due to land–atmosphere feedbacks. Nat. Geosci. 15, 262–268. https://doi.org/10.1038/s41561-022-00912-7

Sen, P.K., 1968. Estimates of the Regression Coefficient Based on Kendall's Tau. Journal of the American Statistical Association 63, 1379–1389. https://doi.org/10.1080/01621459.1968.10480934

Seneviratne, S.I., Nicholls, N., Easterling, D., Goodess, C.M., Kanae, S., Kossin, J., Luo, Y., Marengo, J., McInnes, K., Rahimi, M., Reichstein, M., Sorteberg, A., Vera, C., Zhang, X., Rusticucci, M., Semenov, V., Alexander, L.V., Allen, S., Benito, G., Cavazos, T., Clague, J., Conway, D., Della-Marta, P.M., Gerber, M., Gong, S., Goswami, B.N., Hemer, M., Huggel, C., van den Hurk, B., Kharin, V.V., Kitoh, A., Tank, A.M.G.K., Li, G., Mason, S., McGuire, W., van Oldenborgh, G.J., Orlowsky, B., Smith, S., Thiaw, W., Velegrakis, A., Yiou, P., Zhang, T., Zhou, T., Zwiers, F.W., 2012. Changes in Climate Extremes and their Impacts on the Natural Physical Environment, in: Field, C.B., Barros, V., Stocker, T.F., Dahe, Q. (Eds.), Managing the Risks of Extreme Events and Disasters to Advance Climate Change Adaptation. Cambridge University Press, Cambridge, pp. 109–230. https://doi.org/10.1017/CBO9781139177245.006

Seneviratne, S.I., Zhang, X., Adnan, M., Badi, W., Dereczynski, C., Di Luca, A., Vicente-Serrano, S.M., Wehner, M., Zhou, B., 2021. 11 Chapter 11: Weather and climate extreme events in a changing climate.

Sharma, S., Mujumdar, P., 2017. Increasing frequency and spatial extent of concurrent meteorological droughts and heatwaves in India. Sci Rep 7, 15582. https://doi.org/10.1038/s41598-017-15896-3

Siegmund, J.F., Siegmund, N., Donner, R.V., 2017. CoinCalc —A new R package for quantifying simultaneities of event series. Computers & Geosciences 98, 64–72. https://doi.org/10.1016/j.cageo.2016.10.004

Subash, N., Sikka, A.K., 2014. Trend analysis of rainfall and temperature and its relationship over India. Theor Appl Climatol 117, 449–462. https://doi.org/10.1007/s00704-013-1015-9

Taxak, A.K., Murumkar, A.R., Arya, D.S., 2014. Long term spatial and temporal rainfall trends and homogeneity analysis in Wainganga basin, Central India. Weather and Climate Extremes 4, 50–61. https://doi.org/10.1016/j.wace.2014.04.005

Tootoonchi, F., Sadegh, M., Haerter, J.O., Räty, O., Grabs, T., Teutschbein, C., 2022. Copulas for hydroclimatic analysis: A practice-oriented overview. WIREs Water 9. https://doi.org/10.1002/wat2.1579

Trenberth, K.E., Dai, A., van der Schrier, G., Jones, P.D., Barichivich, J., Briffa, K.R., Sheffield, J., 2014. Global warming and changes in drought. Nature Clim Change 4, 17–22. https://doi.org/10.1038/nclimate2067

Trenberth, K.E., Shea, D.J., 2005. Relationships between precipitation and surface temperature: PRECIPITATION AND TEMPERATURE RELATIONS. Geophys. Res. Lett. 32, n/a-n/a. https://doi.org/10.1029/2005GL022760

van den Dool, H., 2003. Performance and analysis of the constructed analogue method applied to U.S. soil moisture over 1981–2001. J. Geophys. Res. 108, 8617. https://doi.org/10.1029/2002JD003114

Vázquez, M., Nieto, R., Liberato, M.L.R., Gimeno, L., 2023. Influence of teleconnection patterns on global moisture transport during peak precipitation month. Intl Journal of Climatology 43, 932–949. https://doi.org/10.1002/joc.7843

Wallemacq, P., Below, R., McClean, D., 2018. Economic losses, poverty & disasters: 1998-2017. United Nations Office for Disaster Risk Reduction.

Willmott, C.J., 2000. Terrestrial air temperature and precipitation: Monthly and annual time series (1950-1996). WWW url: http://climate. geog. udel. edu/~ climate/html_pages/README. ghcn_ts. html.

Wu, X., Hao, Z., Zhang, X., Li, C., Hao, F., 2020. Evaluation of severity changes of compound dry and hot events in China based on a multivariate multi-index approach. Journal of Hydrology 583, 124580. https://doi.org/10.1016/j.jhydrol.2020.124580

Wu, Y., Miao, C., Sun, Y., AghaKouchak, A., Shen, C., Fan, X., 2021. Global Observations and CMIP6 Simulations of Compound Extremes of Monthly Temperature and Precipitation. Geohealth 5. https://doi.org/10.1029/2021GH000390

Yatagai, A., Kamiguchi, K., Arakawa, O., Hamada, A., Yasutomi, N., Kitoh, A., 2012. APHRODITE: Constructing a Long-Term Daily Gridded Precipitation Dataset for Asia Based on a Dense Network of Rain Gauges. Bulletin of the American Meteorological Society 93, 1401–1415. https://doi.org/10.1175/BAMS-D-11-00122.1

Yin, J., Gentine, P., Slater, L., Gu, L., Pokhrel, Y., Hanasaki, N., Guo, S., Xiong, L., Schlenker, W., 2023. Future socio-ecosystem productivity threatened by compound drought–heatwave events. Nat Sustain. https://doi.org/10.1038/s41893-022-01024-1

Zhang, L., Singh, V.P., 2019. Copulas and their applications in water resources engineering. Cambridge University Press, Cambridge ; New York, NY.

Zhang, W., Luo, M., Gao, S., Chen, W., Hari, V., Khouakhi, A., 2021. Compound Hydrometeorological Extremes: Drivers, Mechanisms and Methods. Front. Earth Sci. 9, 673495. https://doi.org/10.3389/feart.2021.673495

Zscheischler, J., Seneviratne, S.I., 2017. Dependence of drivers affects risks associated with compound events. Sci. Adv. 3, e1700263. https://doi.org/10.1126/sciadv.1700263

Author Contributions:

Conceptualization : Ravi Kumar Guntu, Bruno Merz, Ankit Agarwal;
Data curation : Ravi Kumar Guntu
Formal analysis : Ravi Kumar Guntu
Funding acquisition : Ravi Kumar Guntu, Ankit Agarwal
Investigation : Ravi Kumar Guntu
Methodology : Ravi Kumar Guntu, Bruno Merz, Ankit Agarwal
Project Administration : Ankit Agarwal
Software : Ravi Kumar Guntu
Supervision : Bruno Merz, Ankit Agarwal
Validation : Ravi Kumar Guntu, Bruno Merz
Writing – original draft : Ravi Kumar Guntu
Writing – review & editing : Bruno Merz, Ankit Agarwal

Declaration of Conflict of Interest:
The authors declare no conflicts of interest relevant to this study.

Highlights

- The likelihood of CDHE occurrence depends strongly on the strength and type of dependence between precipitation and temperature.
- Dependence between low precipitation and high temperature exhibits strong space-time variation.
- Low soil moisture preconditioned by dry extremes contributes to CDHE occurrence and its spatial diversity.
- CDHE frequency shows a 2 to 3-fold rise for some regions for the period 1961-2014.